Pyramidality and Metal-Metal Multiple Bonding: Structural Correlations and Theoretical Study

Fernando Mota,† Juan J. Novoa,*,† Jorge Losada,† Santiago Alvarez,*,† Roald Hoffmann,*,‡ and Jérôme Silvestre‡,§

Contribution from the Departament de Química Física and Departament de Química Inorgànica, Universitat de Barcelona, Diagonal 647, 08028 Barcelona, Spain, and Department of Chemistry, Cornell University, Ithaca, New York 14853-1301

Received February 1, 1993

Abstract: An analysis of structural data for more than 350 dinuclear compounds of the types M_2X_8, M_2X_8L, and $M_2X_8L_2$ (M = Cr, Mo, W, Tc, Re, Os, or Rh), with a multiple bond between the transition-metal atoms M, shows the existence of a clear correlation between the average pyramidality angle (M-M-X, or α) and the metal-metal bond distance. Although the presence of axial ligands (L) favors elongation of the M-M bond, this effect is also intimately connected with changes in the pyramidality angle. The metal-metal bond distance also varies with the internal rotation angle, being shorter for the eclipsed conformation in quadruply bonded complexes, while the opposite trend appears for the triply bonded ones. These regularities may help in understanding some apparent inconsistencies previously found in bond order-bond length relationships in multiply bonded metal systems. Electronic structure calculations carried out on simplified model compounds at different levels of sophistication (extended Hückel, Hartree-Fock SCF, and multiconfiguration CASSCF) nicely reproduce the experimental trends and allow us to explain the effect of the different structural parameters on the M-M bond distances.

1. Introduction

The preparation and study of transition-metal complexes with multiple metal-metal bonds constitutes one of the most celebrated innovations, and justly so, in the realm of chemistry during the last decades. The most common compounds of this type are those with the M_2X_8 stoichiometry[1] and their adducts with one or two additional ligands in axial positions, M_2X_8L and $M_2X_8L_2$. The essential geometrical parameters of the LX_4MMX_4L system shown in **1** are the M-M (d) and M-X bond distances, the

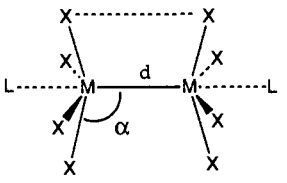

1

"pyramidality" of the MX_4 group, defined by the average M-M-X angle α, the nonbonded X···X distance, and the average internal rotation angle χ (0° for an eclipsed molecule, 45° for the staggered conformation).

Although double and triple bonds are common in organic chemistry, the existence of quadruple bonds was unprecedented. F. A. Cotton and co-workers have shaped this field from its infancy to its present maturity and have introduced the majority of new compounds and the most significant bonding considerations to the chemical community. Some aspects of the conceptual structure of metal-metal multiple bonding formed in the last years still remain puzzling, e.g., the large variability of the quadruple bonds, particularly the supershort Cr(II)-Cr(II) bonds, and their response to axial ligation. Also some inconsistencies have been found in the bond order-bond distance relationships: in the $[Tc_2Cl_8]^{n-}$ family, the Tc-Tc bond distance[2] in the quadruply bonded anion $[Tc_2Cl_8]^{2-}$, 2.151(1) Å, is longer than that in the three salts[3-5] of $[Tc_2Cl_8]^{3-}$ with bond order 3.5: 2.105(1), 2.13-(1), and 2.117(2) Å. A still shorter distance of 2.044(1) Å appears in the Tc_2Cl_8 units present in the extended structure of $K_2[Tc_2Cl_6]$ reported by Kryuchkov *et al.*[6] for what is formally a triple bond. Another series of M-M bonds showing anomalies in the bond order-bond distance relationship is the one formed by three phosphine compounds of general formula $[Re_2Cl_4(PMe_2Ph)_4]^{n+}$ (n = 0, 1, 2). The Re-Re bond orders in these compounds are formally 3.0, 3.5, and 4.0, but the bond distances are 2.241(1), 2.218(1), and 2.215(2) Å, respectively,[7] i.e., the addition of an electron to the δ^* orbital produces an increase of only 0.003 Å in the Re-Re distance, whereas addition of the second δ^* electron stretches the bond by 0.023 Å. This trend has been explained as due to the contraction of the metal d orbitals upon increase of the oxidation state.[8] Finally, some anomalies have been detected in the excited-state geometries of several multiply bonded compounds.[9,10]

In a preliminary account of this work,[11] we showed that a clear

† Universitat de Barcelona.

‡ Cornell University.

§ Current address: Rhône-Poulenc Agrochimie, 14-20 rue Pierre Balzet, 6900 Lyon, France.

(1) (a) Cotton, F. A.; Walton, R. A. *Multiple Bonds Between Metal Atoms*, 2nd ed.; Clarendon Press: Oxford, 1993. (b) Cotton, F. A.; Walton, R. A. *Struct. Bonding (Berlin)* **1985**, *62*, 1 and references within. (c) Chisholm, M. M., Ed. Reactivity of Metal-Metal Bonds. *ACS Symp. Ser.* **1981**, *155*. (d) Poli, R. *Comments Inorg. Chem.* **1992**, *12*, 285. For recent compilations of structural data for Re binuclear compounds, see: (e) Holloway, C. E.; Melnik, M. *Rev. Inorg. Chem.* **1989**, *10*, 235. (f) Kotel'nikova, A. S. *Sov. J. Coord. Chem.* **1991**, *17*, 459; *Koord. Khim.* **1991**, *17*, 867.

(2) Cotton, F. A.; Daniels, L.; Davison, A.; Orvig, C. *Inorg. Chem.* **1981**, *20*, 3051.

(3) Cotton, F. A.; Davison, A.; Day, V. W.; Fredrich, M. F.; Orvig, C.; Swanson, R. *Inorg. Chem.* **1982**, *21*, 1211.

(4) Bratton, W. K.; Cotton, F. A. *Inorg. Chem.* **1970**, *9*, 789.

(5) Cotton, F. A.; Shive, L. W. *Inorg. Chem.* **1975**, *14*, 2032.

(6) Kryutchkov, S. V.; Grigor'ev, M. S.; Kuzina, A. F.; Gulev, B. F.; Spitsyn, V. I. *Dokl. Akad. Nauk SSSR* **1986**, *288*, 389; *Dokl. Chem.* **1986**, *288*, 147. Cotton, F. A.; Daniels, L. M.; Falvello, L. R.; Grigoriev, M. S.; Kryutchkov, S. V. *Inorg. Chim. Acta* **1991**, *189*, 53.

(7) Cotton, F. A.; Dunbar, K. R.; Falvello, L. R.; Tomas, M.; Walton, R. A. *J. Am. Chem. Soc.* **1983**, *105*, 4950.

(8) See ref 1b, p 42.

(9) Schoonover, J. R.; Dallinger, R. F.; Killough, P. M.; Sattelberger, A. P.; Woodruff, W. H. *Inorg. Chem.* **1991**, *30*, 1093.

(10) Lichtenberger, D. L.; Johnston, R. L. In *Metal-Metal Bonds and Clusters in Chemistry and Catalysis*; Fackler, J. P., Jr., Ed.; Plenum Press: New York, 1990.

(11) Losada, J.; Alvarez, S.; Novoa, J. J.; Mota, F.; Hoffmann, R.; Silvestre, J. *J. Am. Chem. Soc.* **1990**, *112*, 8998.

0002-7863/93/1515-6216$04.00/0

Table I. Least-Squares Parameters of eq 1 for Several Families of Dinuclear Complexes with M–M Triple and Quadruple Bonds[a]

metal	ligand	bond order	b	c	r	d_{min}	d_{max}	α_{min}	α_{max}	σ (Å)	no. of data sets
Cr	chelates	4	2.241	3.740	0.996	1.83	2.60	85.2	96.6	0.020	52
Cr	unsupported	4	3.138	3.847	0.998	1.98	3.63	82.7	109.1	0.071	5
Mo	chelates	4	2.158	1.774	0.845	2.06	2.14	91.3	93.0	0.009	62
	carboxylates	4	2.229	4.282	0.827	2.08	2.14	91.3	91.9	0.008	43
	N,N- or N,O-chelates	4	2.164	1.860	0.899	2.06	2.11	92.0	93.0	0.006	19
Mo	carboxylate + phosphine	4	2.131	0.189	0.945	2.09	2.12	94.2	101.0	0.003	7
W	chelates	4	2.222	1.873	0.878	2.16	2.24	89.9	92.1	0.013	21
W	amides	3	2.007	−1.536	0.997	2.29	2.33	100.6	104.5	0.001	5
W	chelate + alkyl	3	2.188	−0.466	0.985	2.19	2.30	90.2	105.2	0.008	8
Mo	halide + phosphine	4	2.191	0.197	0.874	2.12	2.16	102.8	109.3	0.004	13
Mo	propyldiphosphines[b]	4	1.997	−0.568	0.942	2.13	2.16	103.0	106.4	0.005	6
Re	halides	4	2.337	0.455	0.707	2.20	2.30	98.3	110.0	0.015	34
Re	bis(chelate)	4	2.361	1.158	0.853	2.18	2.26	95.9	99.2	0.012	15
Re	tris(chelate)	4	2.336	1.649	0.985	2.20	2.30	92.8	94.7	0.007	3
Re	tetrakis(chelate)	4	2.232	1.509	0.851	2.21	2.25	89.5	90.8	0.010	5
Re	diphosphines[c]	3	2.379	0.562	0.941	2.23	2.31	97.8	106.0	0.012	8
Rh	chelates	1	2.299	2.934	0.840	2.36	2.49	86.5	89.1	0.014	103
Rh	metalated phosphines	1	2.474	2.481	0.881	2.47	2.56	88.0	89.1	0.019	6

[a] b is the *intrinsic* metal-metal bond distance, c is the susceptibility to pyramidalization, r is the regression coefficient, and σ is the standard error of the estimate. [b] Only compounds with rotation angle $\chi \approx 20°$. [c] All compounds with staggered conformation ($\chi > 30°$).

correlation exists between the pyramidality angle α and the Cr–Cr bond distance for a large number of Cr(II) compounds and that a similar correlation could be found for complexes of other transition metals with triple or quadruple M–M bonds. The simple explanation proposed for this effect is based on the enhancement of the valence orbital hybridization upon pyramidalization, supported by the results of molecular orbital calculations. In the following sections we will first discuss in more detail the structural correlations found for a variety of transition metals; these correlations have been obtained from a structural database search guided by the above model. Next we try to explain some of the resulting trends by means of molecular orbital studies (ranging from extended Hückel to CASSCF) on several model compounds. Extrapolation of the structural correlations would result in unrealistically short M–M distances, so we finally address the question of just how short a M–M bond can get.

2. Structural Correlations

2.1 Pyramidality Angle and M–M Bond Distances. Results. We have analyzed the Cambridge Structural Database[12] in search of possible correlations between the structural parameters sketched in **1** (see Methodological Aspects at end of paper for more details). Our search included compounds with M_2X_8, M_2X_8L, and $M_2X_8L_2$ cores for the following metals (metal–metal bond order in parentheses): Cr (4), Mo (4), W (3, 4), Re (3, 4), and Os (3). Compounds of a particular metal and oxidation state were grouped in families having similar ligands, and the results of the least-squares fitting of the average pyramidality angle α and the M–M bond distance d to eq 1 are presented in Table I. Special care

$$d(\mathrm{M–M}) = b + c\cos\alpha \qquad (1)$$

was taken to include only eclipsed or only staggered compounds in a particular family, in order to clearly separate the effects of α and χ.

In eq 1, b corresponds to the expected M–M distance for a compound with $\alpha = 90°$, hereafter referred to as the *intrinsic* bond distance, whereas c gives a measure of the susceptibility of the M–M bond length to pyramidalization.

In the following paragraphs we give a brief description of the criteria used to define different families of complexes. The compounds which do not conform to the general behavior of the corresponding family are singled out, and an explanation for the abnormal behavior is given when possible.

Chromium(II) Chelates. The 51 compounds with quadruple Cr–Cr bonds analyzed can be found listed in the supplementary material (Table A1). All of them correspond to complexes with bridging ligands of the type YXY, where X = C, N, and Y = O, N (with appropriate substituents). Some Cr(II) complexes not included in this analysis are (a) those with a noneclipsed configuration;[13] (b) those having Li^+ ions relatively close to the Cr–Cr bond;[14–16] and (c) organometallic complexes.[14,15,17] In one of the carboxylato compounds,[18] the average α is too large because one of the angles strongly deviates from the average (111° as compared to an average of 99.2°); if this angle is disregarded, the experimental value (1.870 Å) fits well with the least-squares equation. A similar situation occurs with the compound synthesized by Gambarotta and co-workers,[19] in which the chelating ligand is the 7-azaindolyl group: the Cr–Cr–N angle formed by the pyridine nitrogen atoms ($\alpha = 85.2°$) fits well with the least-squares line (experimental Cr–Cr distance = 2.604 Å), but the corresponding angle of the pyrrolidinic nitrogen (88.4°) deviates from the expected behavior, probably a result of the rigidity of the ligand and a misalignment of the lone-pair orbital with the N–Cr bond direction.

Molybdenum(II) Chelates. The 63 molybdenum(II)-containing molecules analyzed give a poorer correlation than found for chromium(II) compounds. However, if only carboxylates are grouped together, and chelates with one or two nitrogen donors are considered separately, the trend becomes much clearer (Table I). Six carboxylates deviate from the typical behavior, and these are marked with an asterisk in Table A2 (supplementary material); one of them corresponds to a ferrocenecarboxylate (identified by the Cambridge database *refcode*, or reference code, fikpiy). Another compound which deviates from the typical behavior, $[Mo_2(carbox)_3(pyCH_2)]$, forms only three chelate rings with carboxylato groups and the fourth one is a metallabicycle. In the family of the N,N- and N,O-chelates (Table A3 in the supplementary material), the molecule identified by the refcode acpimo has the N,O-chelating ligand in a nonbridging coordination mode, hence introducing some strain. Also, the two independent molecules in the compound with refcode bevcou, in which the chelating ligand is xylylacetamido, deviate from the typical behavior; this deviation may be attributed to steric problems between the xylyl groups in the equatorial ligands and the

(12) Allen, F. H.; Kennard, O.; Taylor, R. *Acc. Chem. Res.* **1983**, *16*, 146.
(13) Cotton, F. A.; Rice, G. W.; Sekutowski, J. C. *Inorg. Chem.* **1979**, *18*, 1143.
(14) Krause, J.; Schödl, G. *J. Organomet. Chem.* **1971**, *27*, 59.
(15) Krause, J.; Marx, G.; Schödl, G. *J. Organomet. Chem.* **1970**, *21*, 159.
(16) Cotton, F. A.; Koch, S. *Inorg. Chem.* **1978**, *17*, 2021.
(17) Aoki, T.; Furusaki, A.; Tomiie, Y.; Ono, K.; Tanaka, K. *Bull. Chem. Soc. Jpn.* **1969**, *42*, 545.
(18) Cotton, F. A.; Mott, G. N. *Organometallics* **1982**, *1*, 302.
(19) Edema, J. J. H.; Gambarotta, S.; Meetsma, A.; Bolhuis, F. van; Spek, A. L.; Smeets, W. J. J. *Inorg. Chem.* **1990**, *29*, 2147.

tetrahydrofuran molecules in axial positions, since the analogous compounds with only one axial ligand (bevcua and bevdah) are well behaved.

Tungsten(II) Chelates. Again, the correlation for the whole set of tungsten(II) chelates (data in Table A4) is just fair. If the analysis is limited to the carboxylates, a better correlation results (r = 0.928). In the subfamily of the aminopyridine and hydroxypyridine derivatives, the bond lengths at the shortest end of the family and the pyramidality angle vary little, and any attempt to establish a correlation is meaningless. For the small variability of M–M with α for the shortest bonds, see the discussion on nonlinearity of the $d(\alpha)$ relationship below, as well as the theoretical analysis.

Tungsten(I) Amides. This is a small family so far (Table A5), but the overall variation of the W–W bond distance (0.04 Å) is more than 3 times the estimated standard deviation. Only compounds with nearly-eclipsed conformations were included in the least-squares fitting, for reasons to be discussed below. A compound recently reported by Chisholm *et al.* ($[W_2(O^tBu)_4(NHPh)_2(NH_2Ph)_2]$) does not fit into the general trend of this family, a fact which could be attributed to the presence of the butoxide ligands but also to the large differences between the various bonding angles, ranging from 90 to 100°, or the existence of interligand hydrogen bonding. It is noteworthy that the regression line for $d(\cos\alpha)$ for this family has a negative slope, in opposition to the positive slope found for the previous families, a fact which will be discussed below in light of our theoretical results.

Tungsten(I) Organometallic Chelates. The eight compounds in this family (Table A6), with eclipsed conformation, show a wide variety of W–W bond lengths, well correlated with cos α.

Molybdenum(II) Chelate Phosphines (Mixed Ligand Compounds). All compounds of this family (Table A7) are in an eclipsed conformation. The two compounds with siloxide ligands were omitted from the least-squares fitting. One chlorophosphine complex (refcode bijzez) has two angles much larger than the rest, and it follows the general trend of the family if these two angles are disregarded.

Molybdenum(II) Halophosphines. Compounds of this family (Table A8) correspond to the general formula $Mo_2X_4(PR_3)$, where X is a halide or pseudohalide, and all are present in the eclipsed conformation ($\chi < 2°$). Some relatives are also included in Table A8, having alkoxide or alkyl groups instead of halides and one bridging carboxylato group (compound with refcode fumhie), but these were not included in the least-squares fitting shown in Table I.

Molybdenum(II) Propyldiphosphines. The data for this family of compounds are presented in the supplementary material Table A9. Only compounds with approximately the same rotation angle ($\chi \sim 20°$) were included in the least-squares fitting. The iodo compound was also excluded, as it is generally found that steric problems make the iodo compounds deviate from the behavior of analogous chloro and bromo derivatives (see Discussion).

Rhenium(III) Halides. Given the variety of ligands included in this family (Table A10), the correlation between α and d is not very good, but the trend is still clear.

Rhenium(III) Chelates. There are three different subfamilies of rhenium(III) chelates according to the number of chelating ligands present in the molecule. Although compounds with a variety of ligands are grouped in the family of the bis(chelates), a fair correlation between d and α is found. The exceptions, as found for other metal ions, correspond to compounds with alkyl groups bound directly to the metal or with iodo ligands, (Table A11). Few tris- and tetrakis(chelates) (Tables A12 and A13) have been detected, but they follow the expected trend in both cases.

Rhenium(III) Diphosphines. The compounds of this family (Table A14) show varying degrees of internal rotation (χ angle). Only those compounds with an approximately staggered conformation ($\chi > 30°$) were included in the least-squares fitting of structural data to eq 1.

Rhodium(II) Chelates. The collected structural data for more than 100 rhodium(II) compounds, together with a discussion of the effect of pyramidality on the Rh–Rh single bonds, can be found elsewhere.[20]

Discussion. The first corollary of eq 1 is that metal–metal bond distances cannot be compared directly unless the compounds under consideration have approximately the same pyramidality angle. One should compare both the *intrinsic* M–M distances (b in eq 1) and the susceptibility to pyramidalization (c) of different families of compounds. Let us take the broader approach and compare the values of b and c from Table I in what follows.

Not all the fits presented in Table I are as good as those of the Cr(II) chelates. This may be attributed to the variability of the ligands present in a particular family. For instance, the rather poor fit of the Mo(II) chelates is improved when only carboxylates are considered. Also, the chelate compounds of Re(III) present a poor correlation (not shown in Table I), but if they are grouped, e.g., according to the number of chelating ligands, better correlations result. A similar situation is found for the Re(III) halo complexes, for which differences in size and electronegativity of the halogen can account for the rather poor correlation of Table I, as will be discussed below.

It is surprising that such good correlations are found using the average value of α, given the large differences between the nonequivalent angles of each molecule. There are only a few "pathological" molecules, for which one or two angles are too different from the rest, and in which α correlates well with d only if such angles are disregarded. Such cases are enumerated in the Structural Correlations section, and a qualitative explanation of this fact is given in the theoretical part.

The most remarkable sets of compounds are those with *chelating* ligands, i.e., the carboxylates and their topological analogues in which one or more of the three bridging atoms is replaced by a nitrogen atom. These compounds, in general, show a smaller range of pyramidality angles (variations of α within each family are smaller than 3°, except for Cr(II), for which α varies by 10°) but a much larger angle dependence than all other families of ligands. The Cr(II) chelates seem to be unique in that they are the only compounds to have *both* a wide range of pyramidality angles *and* a strong angle dependence. The chelating carboxylates and analogous ligands apparently favor shorter M–M distances, as can be seen in the trend of the intrinsic distances for the Re(III) complexes, which decrease with the number of chelating ligands (Table I), a trend which has also been found for the Rh(II) chelates.[20] Notice also that the lines $d(\cos\alpha)$ for the families of bis-, tris-, and tetrakis(chelates) of Re(III) are practically parallel.

It is interesting to analyze the trends in the intrinsic M–M distance and in the susceptibility to pyramidalization along a group of the periodic table. For that purpose we can focus on the quadruply bonded chelates of the group 6 metals. The least-squares parameters for the Mo(II) carboxylates must be taken with caution, because the range of experimental values of α is rather small (0.6°). What is striking is that the intrinsic Cr–Cr distance is longer than the Mo–Mo and W–W ones (see Figure 1). Still more striking, the Mo and W compounds have shorter M–M distances than the Cr analogues with a slightly larger α. However, the Cr–Cr distances are shorter than the Mo–Mo (W–W) ones for angles larger than 92.4° (90.6°). In Figure 1 it is seen that the $d(\alpha)$ behavior of the Mo(II) carboxylates may be approximated roughly with the corresponding equation for Cr(II) carboxylates (Table I). Hence, the estimated Cr–Mo bond distance in the heterometallic acetate[21,22] with an average α of 92.3° is 2.091 Å, in good agreement with the experimental value

(20) Aullón, G.; Alvarez, S. *Inorg. Chem.*, in press.
(21) Garner, C. D.; Senior, R. G.; King, T. J. *J. Am. Chem. Soc.* **1976**, *98*, 3526.

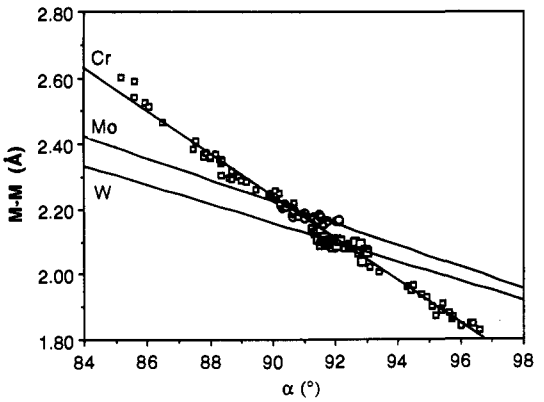

Figure 1. Plot of the experimental M–M distances as a function of the average pyramidality angle α for the families of type $[M_2(chel)_4]$, where M = Cr (■), Mo (□), and W (○), and chel = chelating ligand.

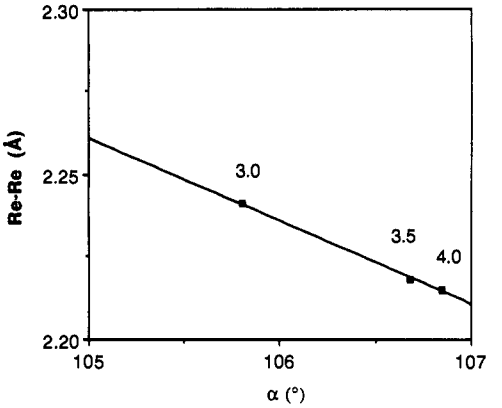

Figure 2. Re–Re distances as a function of the pyramidality angle in the family of compounds with formula $[Re_2Cl_4(PMe_2Ph)_4]^{n+}$ with Re–Re bond orders 3 (n = 0), 3.5 (n = 1), and 4 (n = 2).

of 2.050 Å and sensibly shorter than the Cr–Cr distance in $[Cr_2(AcO)_4]$ (2.26 Å)[23] with an average α of 90°.

Although the number of families analyzed in Table I is not sufficiently large to draw definitive conclusions on the relative importance of the pyramidality effect for different types of ligands, one may tentatively conclude that the intrinsic M–M distance for a particular metal and oxidation state varies in the order

intrinsic M–M distance:

halides > chelates > alkyls > amides

whereas the slopes of the $d(\alpha)$ curves follow a somewhat different ordering:

slope (c) of $d(\alpha)$ curve:

chelates > halides > phosphines ~ alkyls > amides

It is remarkable that in the family of the Mo(II) chelates the substitution of one nitrogen for one oxygen atom in a carboxylate produces drastic variations (see cautionary remark about the data for Mo chelates above) both in the intrinsic distance and in the α dependence. We will come back to this problem later. Another remarkable feature can be found in the families of W(I) complexes containing amide and alkyl ligands, respectively, for which the slope of the least-squares line is negative. Apparently, the pyramidality effect is opposite that found for most complexes, a pathology that we will try to explain in the next sections.

A further corollary of the trends displayed in Table I is that differences in the bond angles can account for the different elongation of the Re–Re bond in the series $[Re_2Cl_4(PMe_2Ph)_4]^{n+}$, hence explaining the apparent anomaly in the bond order–bond distance relationship (Figure 2). The alternative and plausible explanation proposed by Cotton on the basis of the contraction of the d orbitals upon oxidation cannot, however, be ruled out.[7,24]

Another interesting case which can be analyzed in the light of the above structural correlations is the reversible cleavage of the Cr–Cr quadruple bonds in $[Li(thf)]_4[Cr_2Me_8]$ reported by Gambarotta and co-workers.[25] The large pyramidality angle (106.9°) in this compound is consistent with a short Cr–Cr distance (1.980 Å). Although this distance is longer than would be expected from extrapolation of the least-squares fitting for the Cr(II) chelates (Table I), we have already shown that M–M distances at a given α are sensibly shorter for the chelate families than for unbridged compounds. Taking into account the expected dependence of d on α, pulling the two Cr atoms apart should produce a decrease in α, and vice versa. Gambarotta *et al.* chemically reached the other end of the $d(\alpha)$ curve by varying the countercation, breaking the Cr–Cr bond, and obtaining a square-planar, mononuclear species which can be thought of as a dimer with a very long Cr–Cr distance and a pyramidality angle of 90°. Maybe with different countercations one could obtain snapshots along the cleavage reaction coordinate.

Table II. Minimum Distances Expected for Different Families of Dinuclear Compounds (d_{calcd})[a] and Shortest Experimental Distances (d_{expt})[b]

metal	ligand	bond order	r_1	r_2	α_{calcd}	α_{expt}	d_{calcd}	d_{expt}
Cr	unsupported	4	0.997	1.00	116.5	109.1	1.88	1.98
Mo	chelates	4	0.845	0.865	93.1	92.8*	2.07	2.06
	carboxylates	4	0.827	0.826	92.7	91.9	2.06	2.08
	N,N- or N,O-chelates	4	0.899	0.899	99.5	93.0	1.97	2.06
W	chelates	4	0.878	0.931	91.8	92.1	2.16	2.16
Mo	halophosphine	4	0.874	0.877	113.3	101.3	2.12	2.12
Re	halides	4	0.707	0.762	109.4	98.3	2.20	2.23
Re	diphos (χ > 30°)	3	0.941	0.994	106.1	104.3*	2.23	2.23
Rh	chelates	1	0.840	0.861	89.8	89.1*	2.37	2.36

[a] As obtained from a second-order least-squares fitting of the structural data. [b] α_{calcd} is the angle for which the shortest distance in a family can be expected, and α_{expt} is the average experimental pyramidality angle corresponding to the shortest reported distance in a family. The regression coefficients for the first- and second-order fittings are represented by r_1 and r_2, respectively. Asterisks indicate the experimental angles corresponding to the shortest experimental M–M distances where larger angles produce no further shortening of the M–M bond.

Notice that extrapolation of eq 1 for large angles would predict unreasonably short M–M distances. Obviously, for some value of α every family of compounds should reach a minimum distance. This tendency is obvious for the Mo(II) and W(II) complexes (Figure 1), but significant curvature of the $d(\cos\alpha)$ function can also be seen in most of the families with positive susceptibility to pyramidalization (parameter c in Table I). This is indicated by the differences between the regression coefficients of the linear and quadratic least-squares fittings of the M–M bond distances as a function of cos α (Table II). For such families, one can estimate the minimum predicted M–M distance from the least-squares parabola, as shown in Table II.

Let us stress that for three families (marked with asterisks in Table II) a minimum in the $d(\cos\alpha)$ curve appears to have been already experimentally realized, whereas for two other families (Mo(II) N,O- and N,N-chelates and Rh(II) chelates) the least-squares parabola suggests that still shorter distances could be attained.

2.2 Geometrical Aspects of the Ligand Cage. For carboxylato, amidinato, and similar rigid bridging ligands, the bite (X···X)

(22) For a theoretical study of metal–metal bonding in the heterometallic Cr–Mo acetate, see: Wiest, R.; Strich, A.; Bénard, M. *New. J. Chem.* **1991**, *15*, 801.

(23) Cotton, F. A.; Feng, X.; Kibala, P. A.; Matusz, M. *J. Am. Chem. Soc.* **1988**, *110*, 2807.

(24) For a discussion on this point, see: Korol'kov, D. V. *Sov. J. Coord. Chem.* **1991**, *17*, 775; *Koord. Khim.* **1991**, *17*, 1455.

(25) Hao, S.; Gambarotta, S.; Bensimon, C. *J. Am. Chem. Soc.* **1992**, *114*, 3556.

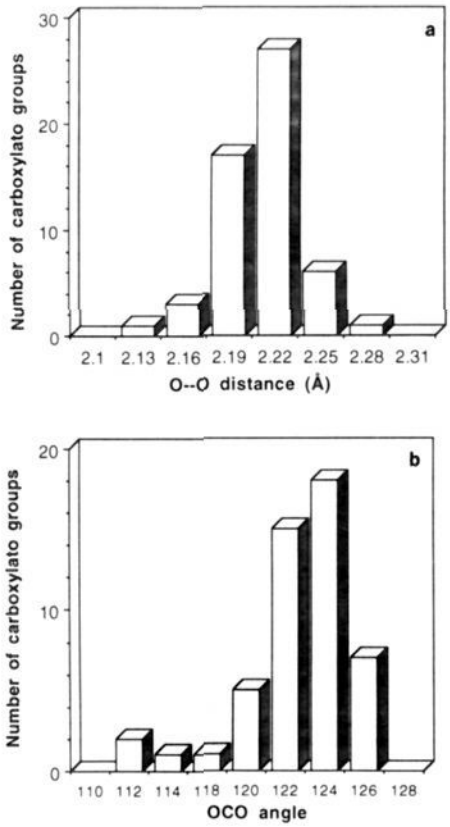

Figure 3. Histograms for the distribution of the O···O distance (a) and OCO bond angles (b) of the carboxylato groups in dinuclear Cr(II) carboxylates.

and the metal–ligand (M–X) distances in **1** are practically constant, whereupon a geometrical relationship between the M–M distance and the pyramidality angle α results:

$$d = X\cdots X + 2(M\text{–}X)\cos\alpha \qquad (2)$$

In fact, most of the Cr(II) dinuclear complexes bear chelating ligands. Hence one could consider such ligands to provide a rigid matrix for the two metal atoms, allowing changes in α to occur only at the expense of modifying M–M. In other words, the correlation between M–M and α could be just a geometrical relationship resulting from the rigidity of the bridging ligands. One can also imagine[26] monodentate ligands brought to a short distance (X···X distance in **1**) by the metal atoms, with lone-pair repulsions preventing them from coming closer, actually providing a set of close-packed anions with approximately constant ligand-ligand distances. In both cases the rigid ligand cage would imply that the M–M distance and α are not independent but are related through eq 2 in the absence of any electronic effect.

It is easy to check whether the rigid ligand cage hypothesis is valid just by looking at the ligand-ligand distances in a series of analogous compounds. Since nonbonded interatomic distances are usually missing in the literature, we used the Cambridge Structural Database[12] to gather the necessary structural information. Histograms for the distribution of nonbonded O···O distances and the O–C–O bond angles of 49 independent carboxylato groups in 11 Cr(II) dinuclear complexes included in our least-squares fitting (Table I) are presented in Figure 3. Although most of the O···O distances and O–C–O angles appear in a narrow range, there is indeed a large range of values for these parameters, indicating that the chelating ligands are quite flexible.

On the other hand, the least-squares fitting of the structural data to eq 1 gives values of b and c far from reasonable estimates

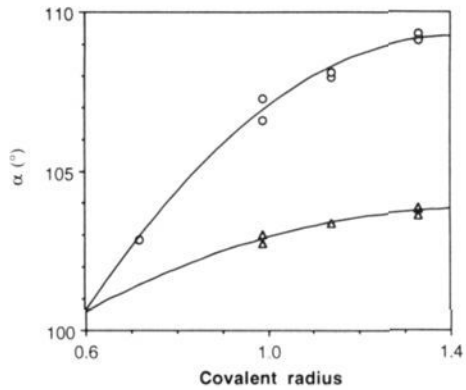

Figure 4. Variation of the pyramidality angle α as a function of the covalent radii of the halide ligands in the compounds of formula $[Mo_2X_4(PMe_3)_4]$ (○) and $[Mo_2X_4(dppm)_2]$ (△).

for X–X and 2(M–X) in eq 2. We conclude that the correlation between the structural data represented by eq 1 cannot be explained solely on the basis of the geometrical constraints of a rigid ligand cage (eq 2). At least part of this dependence can be ascribed to the orbital effect mentioned above, to be discussed in detail below.

Another obvious effect which may be detected is steric repulsion between ligands. A bulkier ligand tries to avoid steric repulsions by adopting a larger angle α without shortening the M–M distance. Two examples can be seen in Figure 4, where the average bond angle for two series of halide–phosphine complexes is plotted against the covalent radii of the halide ligands. This confirms the idea that only compounds with closely related ligands must be analyzed when studying the correlation between d and α. A good example is provided by the family of Re chelates with quadruple bonds (Table I), for which a rather poor correlation is found. If one considers only compounds with the same number of chelating ligands, however, the correlations become quite clear.

To verify the relative importance of the electronic and geometric effects, it would also be interesting to look at the structural data of a family of compounds with nonbridging equatorial ligands. A few families of compounds of Re and Os with nonbridging ligands exist in which the dependence on α is still significant (see Table I). It is also noteworthy that a similar relationship for carbon-carbon bond distances has been found (for the family of ethane derivatives) both experimentally and computationally.[27]

Unfortunately, unsupported metal–metal-bonded Cr(II) compounds are elusive and, with only a few exceptions,[25,28–31] have not been synthesized so far. Some of these are $[Cr_2(taa)_2]$, $[Li(thf)_4][Cr_2Me_8]$, and $Li_4[Cr_2(C_4H_8)_8]\cdot 4C_4H_{10}$, collected in Table III. These complexes have large pyramidality angles and short distances (remember that unbridged compounds always have longer M–M distances than chelates with the same pyramidality angle). In the case of $[Cr_2(taa)_2]$ we think that the experimental distance (2.101 Å) is a *very* short one for such a compound. We argue as follows (i) The unsubstituted dibenzotetraazaannulene[14] is planar, and so are its coordination compounds.[32] However, the tetramethyl derivative (R = CH_3) presents a saddle-shaped conformation, attributed to interactions between neighboring methyl and benzo groups; the same con-

(26) Hargittai, I.; Hargittai, M. *Mol. Struct. Energ.* **1987**, *2*, 1–35.

(27) Schleyer, P. v. R.; Bremer, M. *Angew. Chem., Int. Ed. Engl.* **1989**, *28*, 1226 and references therein.

(28) Edema, J. J. H.; Gambarotta, S.; van der Sluis, P.; Smeets, W. J. J.; Spek, A. L. *Inorg. Chem.* **1989**, *28*, 3784.

(29) Cotton, F. A.; Czuchajowska, J.; Feng, X. *Inorg. Chem.* **1990**, *29*, 4329.

(30) Edema, J. J. H.; Gambarotta, S.; Meetsma, A.; Spek, A. L. *Organometallics* **1992**, *11*, 2452.

(31) Hao, S.; Edema, J. J. H.; Gambarotta, S.; Bensimon, C. *Inorg. Chem.* **1992**, *31*, 2676.

(32) Melson, G. A., Ed. *Coordination Chemistry of Macrocyclic Compounds*; Plenum Press: New York, 1979; pp 280–286.

Table III. Pyramidality Angles and Cr–Cr Distances for Dinuclear Cr(II) Compounds without Bridging Ligands and for Related Mononuclear Complexes[a]

compound	α (degs)	Cr–Cr (Å)	ref
$[Li(thf)_4][Cr_2Me_8]$	106.9	1.980(5)	15
$[Cr_2(taa)_2]$	104.6	2.101(1)	29, 37
$Li_4[Cr_2(C_4H_8)_8]\cdot 4C_4H_{10}$	109.1	1.975(5)	14
$[Na(thf)]_4[Cr_2(PhO)_8]$	82.7	3.622(1)	37
$[Na(py)]_4[Cr_2(PhO)_8]\cdot C_6H_5CH_3$	82.9	3.634(1)	35
$[Li(tmeda)]_2[CrMe_4]$	90.0	(3.08)	25
$[Cr(Me_2PhO)_4]^{2-}$	90.0	(3.08)	35
$[Cr(o\text{-}Me_2NCH_2C_6H_4)_2py]$	84.4	(3.46)	30

[a] See text. Estimated distance in parentheses (Figure 5).

formation appears in its mononuclear Fe(II) complexes. (ii) There are several dinuclear and one-dimensional complexes[33] of dbtaa with group 10 metals; in all of them the ligand is planar, but still the *shortest* metal–metal distance, corresponding to $[Ni(dbtaa)]_2^{2+}$ with a formal bond order of 1, is long (Ni–Ni = 3.063 Å). (iii) Previous theoretical studies on dinuclear and one-dimensional compounds with macrocyclic compounds, such as phthalocyanines or dithiolenes, clearly show that repulsions between the π-electrons of neighboring ligands prevent the metal atoms from getting close. This shows up in the structures in different ways: rotation or slippage of neighboring fragments and pyramidalization of the metal atoms.[34] The saddle-shape conformation of Me_4-dbtaa in the dinuclear chromium compound is likely to produce strong steric repulsions, which may be compensated by the strong Cr–Cr quadruple bond with a large pyramidality angle. This is why we think that the Cr–Cr bond distance of 2.1 Å in the dbtaa compound may be regarded as a very short one.

Gambarotta and co-workers recently reported[35] two unsupported dinuclear Cr(II) compounds, $[Na(thf)]_4[Cr_2(PhO)_8]$ and $[Na(py)]_4[Cr_2(PhO)_8]\cdot C_6H_5CH_3$. In this case, however, the two Cr atoms are far apart from each other (3.6 Å) and apparently held together through the interaction of the cations with the ligands. What is interesting is that the corresponding points in the $d(\alpha)$ graph are connected with those of the unsupported dimers discussed in the previous paragraph, giving a line parallel to that obtained for the carboxylates and analogous chelates (Figure 5).

2.3 Effect of the Axial Ligands. It is well known[36] that the addition of axial ligands to a M_2X_8 molecule, be they solvent molecules, counterions, or neighboring M_2X_8 molecules, results in a lengthening of the M–M bond. Yet no clear correlation has been found between the number of axial ligands or their distance to the M atom and the M–M bond distance. In a preliminary report,[11] we showed that the Cr–Cr bond distances in Cr(II) dinuclear compounds do not depend directly on the number, nature, or distance of the axial ligands but depend only on the pyramidality angle. The same trend can be found for the other families in Table I, and we have therefore excluded all information regarding axial ligands in that table. A detailed study of the effect of axial ligands has been carried out by us recently[20] for the single bonds between Rh(II) centers.

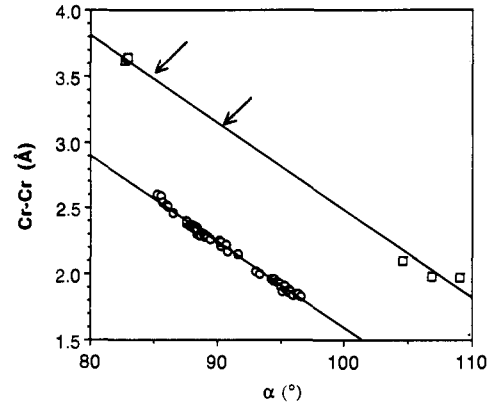

Figure 5. Plot of the Cr–Cr distance as a function of the pyramidality angle α for unbridged Cr(II) dinuclear complexes (□, least-squares line: $d = 9.114 - 0.0663\alpha$; regression coefficient, $r = 0.998$). The corresponding plot for the Cr(II) chelates is also shown (○, least-squares line: $d = 8.079 - 0.0649\alpha$, regression coefficient, $r = 0.997$) for comparison. The arrows indicate the interpolated Cr···Cr distance for a hypothetical dimer of the mononuclear compounds in Table III, assuming the experimental pyramidality angle.

The presence of an axial ligand coordinated to a metal atom, however, favors smaller pyramidality angles, bringing the coordination sphere of M closer to the ideal octahedron. Thus, the axial ligands indirectly favor longer M–M distances by inducing small α. The observation that metal–metal bond cleavage is facilitated by Lewis bases[38] can also be rationalized, taking into account that axial coordination of a Lewis base results in a smaller pyramidality angle and, consequently, a longer (weaker) M–M bond.

2.4 Internal Rotation in Systems with M–M Triple Bonds. From the nature of the metal–metal δ-bonding it is clear that the eclipsed conformation is needed for a quadruple bond to exist in d^4–d^4 compounds. In the staggered conformation the δ-bond is lost. This idea has been elegantly demonstrated through a series of Mo and W compounds[39] with different diphosphines, in which varying degrees of internal rotation appear. The M–M distances in such compounds are clearly correlated with the internal rotation angle.[1]

For triply bonded compounds, on the other hand, free rotation around the M–M bond should be expected on electronic grounds, with possibly the staggered conformation being favored by steric factors.[40] Interestingly, in 10-electron M_2X_8 compounds, a variety of internal rotation angles is found, and the metal–metal distance decreases on going from the eclipsed to the staggered conformation in Tc compounds:[6] in the Tc_2Cl_8 units found in the solid-state structure of $K_2[Tc_2Cl_6]$, the Tc–Tc bond distance is one of the shortest ever reported, 2.044(1) Å,[6,41–43] substantially smaller

(33) (a) Hunziker, M.; Rihs, G. *Inorg. Chim. Acta* **1985**, *102*, 39. (b) Peng, S.-M.; Ibers, J. A.; Millar, M.; Holm, R. H. *J. Am. Chem. Soc.* **1976**, *98*, 8037. (c) Hunziker, M.; Loeliger, H.; Rihs, G.; Hilti, B. *Helv. Chim. Acta* **1981**, *64*, 2544. (d) Hunziker, M.; Hilti, B.; Rihs, G. *Helv. Chim. Acta* **1981**, *64*, 82. (e) Hatfield, W. E. *The Physics and Chemistry of Low-Dimensional Solids*; D. Reidel: Dordrecht, 1980; p 57.

(34) (a) Alvarez, S.; Vicente, R.; Hoffmann, R. *J. Am. Chem. Soc.* **1985**, *107*, 6253. (b) Canadell, E.; Alvarez, S. *Inorg. Chem.* **1984**, *23*, 573.

(35) Edema, J. J. H.; Gambarotta, S.; Van Bolhuis, F.; Spek, A. L. *J. Am. Chem. Soc.* **1989**, *111*, 2142.

(36) See ref 1a, pp 123, 157, 285, and 637; ref 1b, p 23, and also: (a) Cotton, F. A.; Tompson, J. L. *J. Am. Chem. Soc.* **1980**, *102*, 6437. (b) Behling, T.; Wilkinson, G.; Stephenson, T. A.; Tocher, D. A.; Walkinshaw, M. D. *J. Chem. Soc., Dalton Trans.* **1983**, 2109. (c) Cotton, F. A.; Mott, G. N.; Schrock, R. R.; Sturgeoff, L. G. *J. Am. Chem. Soc.* **1982**, *104*, 6781. (d) Cotton, F. A.; Matusz, M. *Inorg. Chem.* **1987**, *26*, 3468.

(37) Edema, J. J. H.; Gambarotta, S.; Van Bolhuis, F.; Smeets, W. J. J.; Spek, A. L. *Inorg. Chem.* **1989**, *28*, 1407.

(38) See ref 29d and also: (a) Hao, S.; Edema, J. J. H.; Gambarotta, S.; Bensimon, C. *Inorg. Chem.* **1992**, *31*, 2676. (b) Wilson, L. M.; Cannon, R. D. *Inorg. Chem.* **1988**, *27*, 2382. (c) Cannon, R. D. *Inorg. Chem.* **1981**, *20*, 3241.

(39) Campbell, F. L.; Cotton, F. A.; Powell, G. L. *Inorg. Chem.* **1984**, *23*, 4222.

(40) Notice that for the d^3–d^3 M_2L_6 complexes (M = Mo, W), the eclipsed structure has been predicted to be more stable than the staggered one due to electronic factors: Albright, T. A.; Hoffmann, R. *J. Am. Chem. Soc.* **1978**, *100*, 7736. The structural data, however, indicate that steric effects may be dominant, since these compounds are practically always staggered: Chisholm, M. H. *Acc. Chem. Res.* **1990**, *23*, 419. Recently, an example of an eclipsed M_2L_6 complex has been structurally characterized: Chisholm, M. H., submitted for publication.

(41) The only shorter Tc–Tc distance known to us appears in the chain compound[42] $[Tc(\mu\text{-}O)_3Tc(\eta^5,\mu\text{-}Cp)]_n$, in which multiple bonding is superimposed on a face-sharing geometry.[43] The compound's structure has been questioned: Herrmann, W. A.; Alberto, R.; Kiprof, P.; Baumgärtner, F. *Angew. Chem., Int. Ed. Engl.* **1990**, *29*, 189; *Angew. Chem.* **1990**, *102*, 208.

(42) Kanellakopulos, B.; Nuber, B.; Raptis, K.; Ziegler, M. L. *Angew. Chem., Int. Ed. Engl.* **1989**, *28*, 1055.

(43) Chan, A. W. E.; Hoffmann, R.; Alvarez, S. *Inorg. Chem.* **1991**, *30*, 1086.

Table IV. Metal–Metal Bond Distances and Rotation Angles for Several Salts of $[M_2X_8]^{n-}$ Ions[a]

compound	bond order	M–M (Å)	χ (deg)	α (deg)	ref
		Os_2X_8			
$(PPN)_2[Os_2Cl_8]$	3	2.212(1)	0.0	103.6(6)	44
brown form[b]	3	2.211(1)	0.0	102.5(6)	44
$(PPN)_2[Os_2Cl_8]$	3	2.206(1)	11.4	103.7(4)	44
green form[b]	3	2.18(2)	39.8	102.8(13)	44
$(Bu_4N)_2[Os_2Cl_8]$	3	2.182(1)	41.0	104.2(3)	45
$(Bu_4N)_2[Os_2Br_8]$	3	2.196(1)	46.7	104.3(4)	45
		Tc_2Cl_8			
$(n\text{-}Bu_4)_2[Tc_2Cl_8]$	4	2.151(1)	0.0	103.8	2
$Y[Tc_2Cl_8]\cdot 9H_2O$	3.5	2.105(1)	15.8	104.3	3
$(NH_4)_3[Tc_2Cl_8]\cdot 2H_2O$	3.5	2.13(1)	0.0	105.1	4
$K_3[Tc_2Cl_8]\cdot nH_2O$	3.5	2.117(2)	0.0	104.8	5
$K_2[Tc_2Cl_6]$	3	2.044(1)	45.0	102.7	6
$(C_5H_5NH)_3[Tc_2Cl_8]$	3.5	2.118		105.2	46
		Re_2X_8			
$(Bu_4N)_2[Re_2F_8]$	4	2.20(1)[c]			47
$(Bu_4N)_2[Re_2Cl_8]$[b]	4	2.224(1)	0	103.4	48
		2.215(2)	0	102.3	
$(Et_4N)_2[Re_2Cl_8]$	4	2.215	0	103.3	49a
$Cs_2[Re_2Cl_8]\cdot H_2O$	4	2.226	0	104.0	49b
$Cs_2[Re_2Br_8]$	4	2.228(4)	0.0	104.6	50
$(Bu_4N)_2[Re_2Br_8]$[b]	4	2.226(4)	0	104.2	51
		2.209(6)	0	103.8	
$[Re_4I_8(CO)_6]$	4	2.279(1)	41.1	101.6	52
$(Bu_4N)_2[Re_2I_8]$	4	2.245(3)	0	105.4	53
$[Re_2I_4(O_2CC_6H_5)_2]$	4	2.198(1)	0	110.0	54

[a] Not included are the data from a structure with large thermal ellipsoids.[26] [b] The two sets of data for this compound correspond to the nonequivalent crystallographic sites. [c] EXAFS data.

than those previously found for the quadruply bonded Tc(III) compound $(Bu_4N)_2[Tc_2Cl_8]$, of 2.151(1) and 2.133(3) Å.[2] A similar effect can be observed for the $[Os_2Cl_8]^{2-}$ ion (see Table IV).

Further experimental evidence for the relationship between the internal rotation angle and the M–M distance has been obtained from vibrational spectra of $[Re_2X_8]^{2-}$ complexes (X = Cl, Br).[9] In a single-crystal, the excited state ($\delta\delta^*$ configuration) preserves the eclipsed geometry of the ground state (δ^2 configuration), and the M–M vibrational frequencies in the vibronic spectra correspondingly decrease from 274 to 249 cm^{-1} (for X = Cl) and from 275 to 252 cm^{-1} (for X = Br). The time-resolved resonance Raman spectra show that in solution the excited state relaxes to a staggered conformation and the Re–Re stretching freuencies become 262 cm^{-1} for both X = Cl and Br. Hence, the triply bonded $\delta\delta^*$ excited state is estimated to have a Re–Re bond distance 0.044 Å shorter in the staggered than in the eclipsed conformation.

Obviously, the internal rotation/bond distance relationships for triple and quadruple metal–metal bonds imply that both angles α and χ must be taken into account when comparing M–M bond distances. Thus, only compounds in an approximately eclipsed conformation (i.e., $\chi < 5°$) were considered so far (Table I). There are a few families in which α is practically constant, and the metal–metal distances can be fitted to eq 3 (Table IV). Finally,

$$d = f + g\cos(2\chi) \quad (3)$$

for those cases in which both α and χ vary, fitting of the structural data to eq 4 summarizes both trends. In eq 4 the standard M–M

$$d = d_0 + i\cos\alpha + j\cos(2\chi) \quad (4)$$

distance d_0 corresponds to a compound with the staggered conformation and $\alpha = 90°$. The least-squares parameters are presented in Table V. Note that the dependence on χ has different sign for the triply and quadruply bonded compounds. Also, notice the different sign of the dependence on α for the phosphine complexes of Mo. This anomaly will be discussed below (see section entitled How Short Can a Metal–Metal Bond Be?).

3. Molecular Orbital Studies

There is vast theoretical literature on M–M multiple bonds,[55] but the pyramidality effect has not been addressed before. In this section we report our theoretical studies on Cr(II), Os(III), and Os(IV) model compounds. Bonding and electronic structure in Cr(II) compounds have been studied at the *ab initio* level by several authors,[56–58] but we are not aware of any calculations concerning Os complexes.

3.1 Cr–Cr Quadruple Bond in Cr_2O_8 and $Cr_2O_8Cl_2$ Cores. Effect of Pyramidalization and Hybridization on M–M Bond Strengths. In order to study theoretically the effect of the pyramidality on the M–M bond strength, it is natural to focus on the family with the strongest pyramidality dependence, that of the Cr(II) carboxylates. Hence, we choose a Cr(II) model compound with oxo ligands, $[Cr_2O_8]^{12-}$. The oxo ligands should provide a coordination environment for the Cr atoms similar to that in the carboxylato complexes, whereas removal of the organic CR fragment from our model compound **2** allows us to focus on the

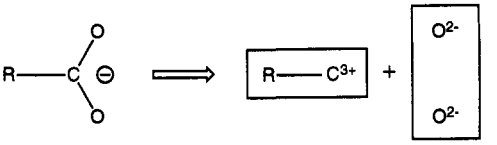

2

effects associated with only the first coordination sphere of the metal atoms and disregard, as a first approximation, the

(44) (a) Fanwick, P. E.; King, M. K.; Tetrick, S. M.; Walton, R. A. *J. Am. Chem. Soc.* **1985**, *107*, 5009. (b) Fanwick, P. E.; Tetrick, S. M.; Walton, R. A. *Inorg. Chem.* **1986**, *25*, 4546.
(45) Agaskar, P. A.; Cotton, F. A.; Dunbar, K. R.; Falvello, L. R.; Tetrick, S. M.; Walton, R. A. *J. Am. Chem. Soc.* **1986**, *108*, 4850.
(46) Grigor'ev, M. S.; Kryutchkov, S. V.; Strutchkov, Y. T.; Yanovskii, A. I. *Koord. Khim.* **1990**, *16*, 90.
(47) Conradson, S. D.; Sattelberger, A. P.; Woodruff, W. H. *J. Am. Chem. Soc.* **1988**, *110*, 1309.
(48) Cotton, F. A.; Frenz, B. A.; Stults, B. R.; Webb, T. R. *J. Am. Chem. Soc.* **1976**, *98*, 2768.
(49) (a) German, K. E.; Grigor'ev, M. S.; Cotton, F. A.; Kryutchkov, S. V.; Falvello, L. *Sov. J. Coord. Chem.* **1991**, *17*, 663; *Koord. Khim.* **1991**, *17*, 1230. (b) Koz'min, P. A.; Novitskaya, G. N.; Kuznetsov, V. G. *Zh. Strukt. Khim.* **1973**, *14*, 680; *J. Struct. Chem.* **1973**, *14*, 629.
(50) Cotton, F. A.; DeBoer, B. G.; Jeremic, M. *Inorg. Chem.* **1970**, *9*, 2143.
(51) Huang, H. W.; Martin, D. S. *Inorg. Chem.* **1985**, *24*, 96.
(52) Calderazzo, F.; Marchetti, F.; Poli, R.; Vitali, D.; Zanazzi, P. F. *J. Chem. Soc., Dalton Trans.* **1982**, 1665.
(53) Cotton, F. A.; Daniels, L. M.; Vidyasagar, K. *Polyhedron* **1988**, *7*, 1667.
(54) Bratton, W. K.; Cotton, F. A. *Inorg. Chem.* **1969**, *8*, 1299.
(55) For a thorough review on this topic, see ref 22.
(56) Bénard, M. *J. Am. Chem. Soc.* **1978**, *100*, 2354.
(57) See, e.g., (a) Davy, R. D.; Hall, M. B. *J. Am. Chem. Soc.* **1989**, *111*, 1268. (b) Ziegler, T. *J. Am. Chem. Soc.* **1985**, *107*, 4453. (c) Hay, P. J. *J. Am. Chem. Soc.* **1978**, *100*, 2898. (d) Hall, M. B. *J. Am. Chem. Soc.* **1980**, *102*, 2104. (e) Bénard, M.; Veillard, A. *Nouv. J. Chim.* **1977**, *1*, 97. (f) Garner, C. D.; Hillier, I. H.; Guest, M. F.; Green, J. C.; Coleman, A. W. *Chem. Phys. Lett.* **1976**, *48*, 587. (g) Bursten, B. E.; Clark, D. L. *Polyhedron* **1987**, *6*, 695. (h) Ziegler, T.; Tachinke, V.; Becke, A. *Polyhedron* **1987**, *6*, 685. (i) Hall, M. B. *Polyhedron* **1987**, *6*, 679. (j) Arriata-Pérez, R.; Case, D. A. *Inorg. Chem.* **1984**, *23*, 3271. (k) Goodgame, M. M.; Goddard, W. A. *J. Phys. Chem.* **1981**, *85*, 215. (m) Atha, P. M.; Hillier, I. H.; Guest, M. F. *Chem. Phys. Lett.* **1980**, *75*, 84. (n) Bursten, B. E.; Cotton, F. A.; Hall, M. B. *J. Am. Chem. Soc.* **1980**, *102*, 6348. (o) Guest, M. F.; Garner, C. D.; Hillier, I. H.; Walton, I. B. *J. Chem. Soc., Faraday Trans. 2* **1978**, *11*, 2092. (p) Hillier, I. H.; Garner, C. D.; Mitcheson, G. R.; Guest, M. F. *J. Chem. Soc., Chem. Commun.* **1978**, 204. (q) Block, T. F.; Fenske, R. F.; Lichtenberger, D. L.; Cotton, F. A. *J. Coord. Chem.* **1978**, *8*, 109. (r) Cotton, F. A.; Kalbacher, B. J. *Inorg. Chem.* **1977**, *16*, 2368. (s) Cotton, F. A. In *Perspectives in Coordination Chemistry*; Williams, A. F., Floriani, C., Mebach, A. E., Eds.; VCH Publishers: New York, 1992.
(58) Hay, P. J. *J. Am. Chem. Soc.* **1982**, *104*, 7007.

Table V. Least-Squares Fitting Parameters for M–M Bond Distances as a Function of Pyramidality and Internal Rotation Angles (eq 5)

metal	ligand	bond order	h	i	j	r	esd	d_{min}	d_{max}	no. of compds
Re	diphosphines	3	2.356	0.507	0.038	0.850	0.022	2.21	2.38	14
Mo	halodiphosphines	4	2.128	–0.210	–0.043	0.892	0.007	2.13	2.18	16
Os	assorted[a]	3	2.315	0.537	0.018	0.924	0.029	2.18	2.39	19

[a] Includes O,O- and N,O-chelates and halides.

geometrical constraints imposed by the rigidity of the bridging ligand. All calculations performed on Cr model compounds were of the extended Hückel type (see computational section for details). One advantage of this approximate molecular orbital method is that it is not sensitive to the net molecular charges, thus the highly charged model compound causes no problems.

Following the usual methodology, we keep the Cr–Cr and Cr–O bond distances constant and study the changes in overlap populations (which scale as bond strengths) with the pyramidality angle α. We have carried out several sets of calculations in which two sets of bond angles were used (D_{2d} point group), differing by as much as 15°. In all cases, the differences in the Cr–Cr overlap population between the different sets of calculations were smaller than 2% for a given average pyramidality angle. This computational result nicely reproduces the experimental finding that structural correlations depend only on the *average* experimental pyramidality angle, as discussed above. In consequence, we vary all the bond angles simultaneously in the sequel.

The basic MO scheme for the M_2X_8 compounds, as calculated for $[Cr_2O_8]^{12-}$, is shown in **3a** for the eclipsed and in **3b** for the staggered conformation. It is a classical quadruple bond picture,

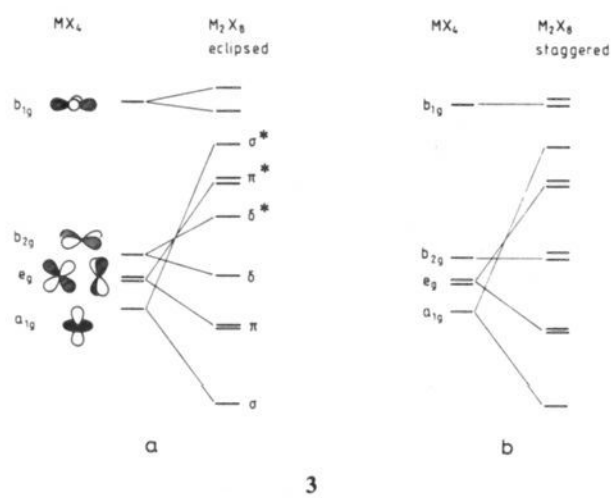

3

as first introduced by Cotton *et al.*[59] For d^4 ions in an eclipsed complex, a $\sigma^2\pi^4\delta^2$ electron configuration results, corresponding to a M–M bond order of 4. On the other hand, the d^6 ions have a bond order of 3 in both the eclipsed and the staggered conformations. The calculated overlap population between the two $(CrO_4)^{6-}$ fragments and also some interatomic overlap populations are presented in Figure 6. There it can be seen that the overlap population between the two $(CrO_4)^{6-}$ fragments increases with α. Two different regions can be identified in Figure 6: for large angles ($\alpha > 100°$), the fragment-fragment overlap population is essentially due to Cr–Cr bonding, whereas for $\alpha < 100°$ lone-pair repulsions between nonbonded atoms contribute also to changes in the fragment-fragment overlap population. Negative overlap populations below –0.05 are a clear indicator of repulsion, according to experience from many extended Hückel calculations.

For the time being we focus only on the Cr–Cr overlap population. The contributions from the σ-, π-, and δ-components

(59) Cotton, F. A.; Curtis, N. F.; Harris, C. B.; Johnson, B. F. G.; Lippard, S. J.; Mague, J. T.; Robinson, W. R.; Wood, J. S. *Science* **1964**, *145*, 1305.

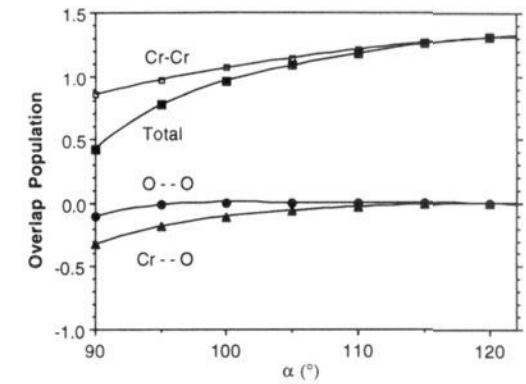

Figure 6. Calculated (EH level) Cr–Cr overlap population (□) at varying pyramidality angles α, compared to the overlap population between the two $(CrO_4)^{6-}$ fragments (■) in the model compound $[Cr_2O_8]^{12-}$. The overlap populations between nonbonded atoms (O···O and Cr···O) are also shown.

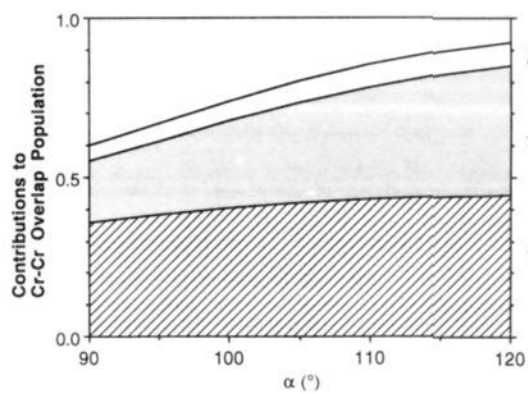

Figure 7. σ, π, and δ contributions to the Cr–Cr overlap population as a function of the pyramidality angle in the model compound $[Cr_2O_8]^{12-}$.

of the overlap population are shown in Figure 7. The largest variation with the pyramidality angle comes from the contribution of the Cr–Cr π-bonds, with the σ-bond contributing a little less than one of the π-bonds. On the other hand, the δ-bond is practically insensitive to changes in α. A consequence of this finding is that the same dependence is to be expected for triple and quadruple bonds.

The orbital explanation for the pyramidality effect is as follows. In a square planar MX_4 ($\alpha = 90°$) fragment, the σ- and π-components of the quadruple bond are composed of pure metal d_{z^2} and d_{xz}, d_{yz}, respectively, assuming no π-bonding with X, as shown in **4**. Upon departure from fragment D_{4h} to C_{4v} symmetry, well-understood mixing (hybridization)[60] with metal $p_{x,y,z}$ orbitals occurs. The net result is stronger σ- and π-components of the quadruple bond as α increases from 90°. We have performed a simple test to probe this assertion: if mixing of the 4p orbitals is turned off by making them highly contracted (i.e., by using a large Slater exponent, $\zeta = 8.0$ instead of the standard value of 1.7 for Cr), the Cr–Cr overlap population becomes practically

(60) (a) Silvestre, J.; Albright, T. A.; Sosinsky, B. A. *Inorg. Chem.* **1981**, *20*, 3937. (b) Elian, M.; Hoffmann, R. *Inorg. Chem.* **1975**, *14*, 1058. (c) Burdett, J. K. *J. Chem. Soc., Faraday Trans. 2* **1974**, *70*, 1599. (d) Böhm, M. C.; Daub, J.; Gleiter, R.; Hofmann, P.; Lappert, M. F.; Öfele, K. *Chem. Ber.* **1980**, *113*, 3629. (e) Hoffmann, R.; Chen, M. M. L.; Elian, M.; Rossi, A. R.; Mingos, D. M. P. *Inorg. Chem.* **1974**, *13*, 2666.

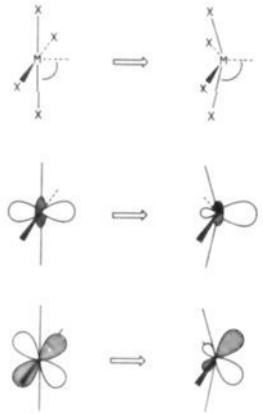

4

invariant with α, as shown in Figure 8. Even if the model employed is highly simplified, our conclusions are in excellent agreement with the large range of Cr–Cr bond distances found experimentally.[10]

Nature of the Ligands. Interesting features of the structural correlations found (Table I) are that the dependence of the M–M distance on α found for the phosphine complexes is smaller than that for carboxylato or halo derivatives and that the amide complexes of W(I) and the halopropyldiphosphine complexes of Mo(II) show an inverted behavior (i.e., the distance increases with increasing α). Since one reason for the differential behavior of different families of compounds might be related to their different π-acceptor/π-donor abilities, we explore now the effect of the π-donor or π-acceptor nature of the ligands on the pyramidality dependence of the M–M bond lengths.

If the oxo ligands in our model compound are replaced by simple σ-donor hydride ligands, the dependence of d on α practically disappears (Figure 9), especially for $\alpha > 100°$. In order to understand the different behavior of a σ-donor ligand, we note first that for small angles a large part of the angle dependence in $[Cr_2O_8]^{2-}$ is due to the nonbonded Cr···O repulsion built into the π-bonding MOs (**5**). This is so since increasing α

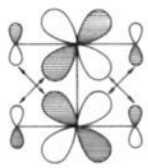

5

decreases the antibonding $p_z(O)/d_{xz}(Cr)$ overlap (indicated by a double-headed arrow in **5**). This effect is obviously missing in the corresponding hydride. On the other hand, the metal d_{xz} and d_{yz} contributions to the orbitals of the CrO_4 fragment involved in Cr–Cr π-bonding increase with α but diminish for the CrH_4 fragment, as seen in Figure 10. Compare the differences in the $d(\alpha)$ curves for Mo(II) carboxylates (π-donor and poor σ-donor) and phosphines (good σ-donor).

Effect of the Axial Ligands. Since the presence of axial ligands has long been recognized as responsible for a lengthening of the Cr–Cr distance, previous efforts to understand bond length variations in the system have focused on the contact to the extra axial ligands L. However, no clear correlation between the Cr–axial ligand and the Cr–Cr bond distance exists.

We analyze theoretically the effect of such axial ligands (at the extended Hückel level) by just adding two chloride ligands to our previous model compound $[Cr_2O_8]^{12-}$. Keeping the

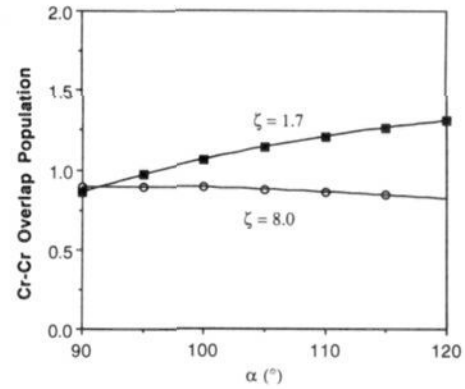

Figure 8. Variation of the Cr–Cr overlap population as a function of the bond angle α, calculated with the standard Slater exponent ($\zeta = 1.7$) for the Cr 4p orbitals and with highly contracted ($\zeta = 8.0$) 4p orbitals.

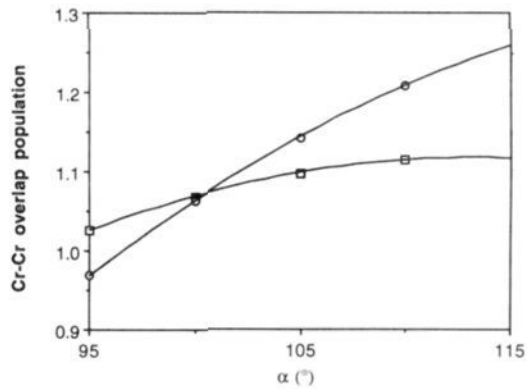

Figure 9. Comparison of the calculated dependence of the Cr–Cr overlap population (EH level) on α for different ligands: O^{2-} (○), H^- (□).

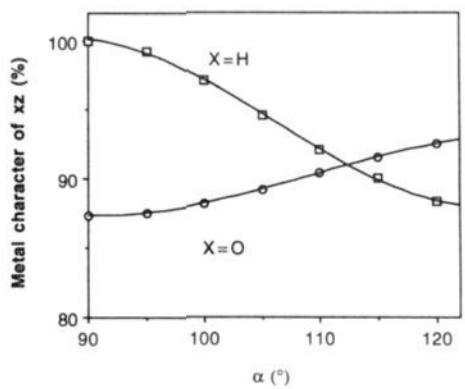

Figure 10. Variation of the metal character of the "xz" MO as a function of α in Cr_2X_8 when $X = O^{2-}$ (○) and $X = H^-$ (□).

geometry of the Cr_2O_8 fragment untouched (with $\alpha = 103°$), the Cr–Cr overlap population is only slightly diminished by the addition of the axial chlorides (Cr–Cl = 2.5 Å): from 0.364 in $[Cr_2O_8]^{12-}$ to 0.346 in $[Cr_2O_8Cl_2]^{14-}$. If the pyramidality angle is then allowed to relax, it becomes smaller (~95°) and the Cr–Cr bond is significantly weakened (overlap population 0.304), as summarized in Figure 11.

In Figure 11, it is also seen that closing the pyramidality angle from 103 to 95° produces an important strengthening of the Cr–Cl_{ax} bond. In fact, the mixing of the d_{z^2} and p_z metal orbitals, which improves the M–M bonding on pyramidalization, is unfavorable for metal–axial ligand bonding, as schematically indicated in **4**. Hence, the angle α is a compromise between the large values required for good M–M bonding and the small values needed for M–Cl_{ax} bonding. In other words, the metal atom prefers an octahedral geometry. On the other hand, the optimum

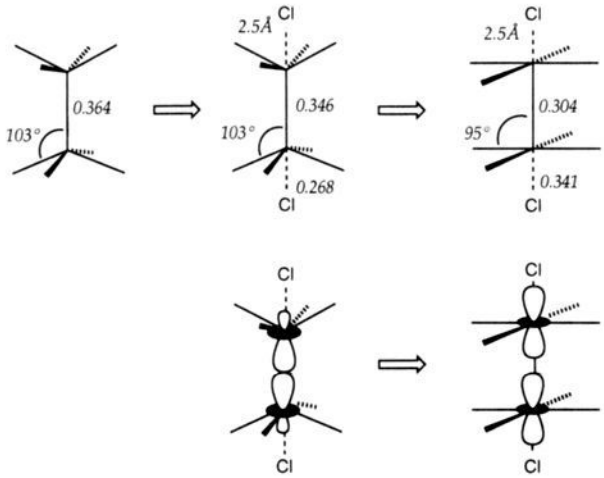

Figure 11. Effect of the addition of an axial ligand to a Cr_2O_8 core (while keeping the pyramidality angle constant) and of decreasing that angle while keeping the axial ligand at a constant distance (top). Schematic representation of the "dehybridization" in the σ MO when the pyramidality degree is reduced, favoring interaction with the axial ligands (bottom). The numbers in italics represent the calculated overlap population (EH) for a particular bond.

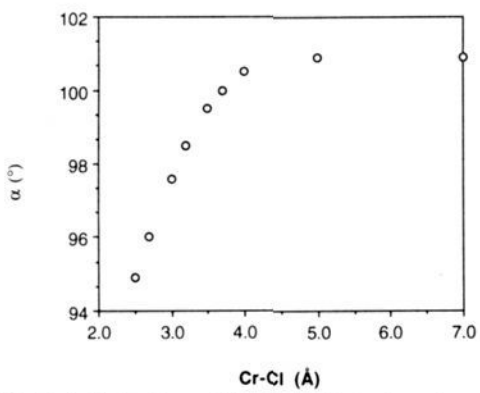

Figure 12. Optimized values of the Cr–Cr–O bond angles α in the $[Cr_2O_8]^{12-}$ core as a function of the distance of two axial chloride ligands to the Cr atoms.

α varies with the distance of the axial ligand to the metal (Figure 12): the closer the axial ligand is, the smaller α becomes.

Since the pyramidality angle itself affects the M–M bond distance as discussed in a previous section, it is clear that the presence of axial ligands indirectly affects the M–M bond distance. The experimental data support this explanation: 51 Cr(II) molecules with two, one, or no axial ligands align themselves along a unique $d(\alpha)$ line (Figure 13). Certainly the compounds with two axial ligands have *in general* smaller angles than those with one, and those without axial ligands have the larger angles. But one can find compounds with, e.g., $\alpha \approx 94°$, with or without axial ligands, having practically the same bond lengths.

Obviously, mixing of the σ lone-pair orbitals of the axial ligands with the M–M bonding and antibonding combinations of the d_{z^2} orbitals may also have some influence on the M–M bond strength, as discussed previously by Bursten *et al.*[61] However, the fact that Cr(II) compounds with two, one, or no axial ligands show a very good correlation between d and α (Figure 1) suggests that the changes in pyramidality are mainly responsible for the M–M bond weakening when axial ligands are present, at least for the

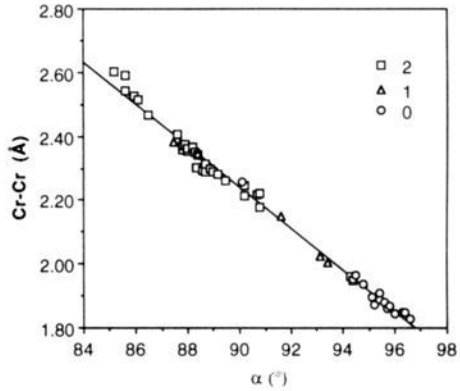

Figure 13. Plot of the Cr–Cr bond distance as a function of the pyramidality angle α for the family of Cr(II) chelates with varying number of axial ligands. The number of axial ligands for each experimental point is indicated in the inset.

cases of Cr(II) (see above, Structural Correlations section) and Rh(II) compounds.[20]

It is tempting at this point to advance an explanation for the reversible cleavage of the Cr–Cr quadruple bonds of $[Cr_2(taa)_2]$ (taa = tetramethyldibenzotetraaza[14]annulene) in pyridine,[31] producing the octahedral compound $[Cr(taa)(py)_2]$. According to Murray-Rust, Bürgi, and Dunitz,[62] "if a correlation can be found between two or more independent parameters describing the structure of a given structural fragment in a variety of environments, then the correlation function maps a minimum energy path in the corresponding parameter space". Therefore, in the light of the present results, a likely pathway for such a reaction would involve axial coordination of pyridine molecules to the dinuclear unit, thus decreasing the pyramidality angle (from 104.6° in the bare dimer to approximately 90° in the pyridine adduct), imposing great strain on the molecule and finally facilitating the cleavage of the Cr–Cr bond and the coordination of an additional pyridine molecule to each Cr atom.[63]

3.2 Os–Os Triple and Quadruple Bonds in Os_2Cl_8 and Os_2Cl_{10} Cores. In order to check the general applicability of our model for the pyramidality effect, depending on hybridization of the metal, as discussed in the previous section for a Cr model compound, we have carried out calculations also for Os(IV) and Os(III) compounds in both the eclipsed and the staggered geometries. Also, to make sure that our theoretical results are not biased by the approximations involved in the extended Hückel methodology, we compare in this section the results at three different levels of sophistication: EH, SCF (Hartree–Fock self-consistent field), and CASSCF (multiconfigurational self-consistent field calculations using a complete active space of configurations). The analogies and differences between SCF and CASSCF results are discussed in more detail in the methodological section.

Effect of Pyramidalization and Hybridization on M–M Bond Strengths. We assume the eclipsed conformation for the quadruply bonded Os(IV) compound $[Os_2Cl_8]$ and the staggered one for the triply bonded Os(III) complex $[Os_2Cl_8]^{2-}$. Let us first note that the MO schemes obtained from EH calculations are qualitatively very similar to those presented above for the Cr_2O_8 core (see **3**). The EH calculations give energy minima at larger α than for the Cr_2O_8 model compound: $\alpha = 101.2$, 106.9, and 105.2° for Cr(II), Os(III), and Os(IV), respectively. This

(61) (a) Bursten, B. E.; Clark, D. L. *Polyhedron* **1987**, *6*, 695. (b) Braydich, M. D.; Bursten, B. E.; Chisholm, M. H.; Clark, D. L. *J. Am. Chem. Soc.* **1985**, *107*, 4459. (c) Chisholm, M. H.; Clark, D. L.; Huffman, J. C.; Van Der Sluys, W. G.; Kober, E. M.; Lichtenberger, D. L.; Bursten, B. E. *J. Am. Chem. Soc.* **1987**, *109*, 6796. (d) Chisholm, M. H.; Clark, D. L.; Huffman, J. C.; Van Der Sluys, W. G. *J. Am. Chem. Soc.* **1987**, *109*, 6817.

(62) Murray-Rust, P.; Bürgi, H.-B.; Dunitz, J. D. *J. Am. Chem. Soc.* **1975**, *97*, 921. For a recent account of the principles and applications of structure correlations, see: Bürgi, H.-B. In *Perspectives in Coordination Chemistry*, Williams, A. F., Floriani, C., Meerbach, A. E., Eds.; Verlag Helvetica Chimica Acta: Basel, 1992.

(63) For the related chromium(III) compound, [Cr(taa)Cl], see: Cotton, F. A.; Czuchajowska, J.; Falvello, L. R.; Feng, X. *Inorg. Chim. Acta* **1990**, *172*, 135.

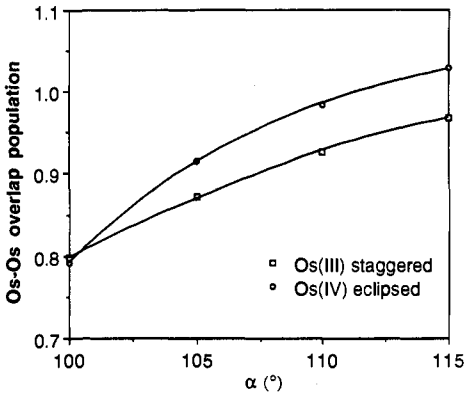

Figure 14. Calculated (EH level) Os–Os overlap population as a function of α for the $[Os_2Cl_8]^{n-}$ complexes of Os(III) (n = 2, □, triple bond, staggered conformation) and Os(IV) (n = 0, ○, quadruple bond, eclipsed conformation).

can be in part attributed to the larger size of the chloride ligands and is consistent with the fact that experimental angles in Os(III) halides are larger than those in Os(III) chelates, in which the donor atoms are O or N. For bond angles close to that of the energy minimum ($100° < \alpha < 110°$), the dependence of the bond strength (Os–Os overlap population) on the pyramidality angle very much resembles that previously found for the Cr(II) complexes (see Figure 14).

In order to check the importance of effects not considered in the extended Hückel methodology, such as two-electron terms and internuclear repulsions, SCF calculations were performed for $[Os_2Cl_8]$ and $[Os_2Cl_8]^{2-}$, models for quadruple and triple bonds, respectively. The highest occupied MOs have the same symmetries and topologies as those found at the EH level. However, it is known that for the correct description of M–M multiple bonds, the inclusion of electron correlation effects is needed,[64] and for that reason we have also performed a series of CASSCF calculations on $[Os_2Cl_8]$ and $[Os_2Cl_8]^{2-}$. A correct description of these systems at the CASSCF level would require the inclusion of both M–M and M–X bonding interactions into the active space. However, the computational effort needed for such an active space is technically unfeasible at present time. Therefore, we have included only the M–M bonding and antibonding orbitals (3) in the active space, in order to attempt an adequate description of the M–M bond. The M–X interactions will be described only in an averaged way. The active space thus contains eight electrons and eight orbitals of symmetries a_{1g}, e_u, b_{2g}, b_{1u}, e_g, and a_{2u} in the eclipsed geometry. For simplicity, we will label these orbitals as σ, π, δ, δ^*, π^*, and σ^* from here on.

The CASSCF occupations of the active orbitals of $[Os_2Cl_8]^{2-}$ in the staggered geometry are $(\sigma)^{1.9}(\pi)^{3.7}(\delta,\delta^*)^4(\sigma^*)^{0.1}(\pi^*)^{0.3}$, corresponding to a calculated bond order of 2.6. The corresponding occupations in the eclipsed conformation are not significantly different. The occupation of antibonding orbitals in a multiconfiguration approach results in weaker M–M bonds than predicted by SCF calculations, as reported previously by Bénard[56] for a Re–Re triple bond. Both at the SCF and CASSCF levels, rotating the molecule from the staggered to the eclipsed conformation induces an energy increase of about 3 kcal/mol.

For $[Os_2Cl_8]$ in the eclipsed conformation, the configuration of the optimized structure is $(\sigma)^{1.9}(\pi)^{3.6}(\delta)^{1.4}(\delta^*)^{0.5}(\pi^*)^{0.5}(\sigma^*)^{0.1}$. The calculated bond order of 3.0 is somewhat larger than that for the Os(III) compound (let us recall that the formal bond orders are 3 and 4 for Os(III) and Os(IV), respectively). The occupations of the virtual orbitals are practically invariant with α but increase with increasing Os–Os distance as a result of the decreasing energy gap between the bonding and antibonding orbitals. All these results corroborate the need for a multireference approach in order to achieve a correct quantitative description of the M–M multiple bond, as previously found by Hay[56] for $[Re_2Cl_8]^{2-}$.

Some of the parameters optimized at the SCF and CASSCF levels (see computational section for details) are presented in Table VI. The optimized pyramidality angle for $[Os_2Cl_8]$ in the eclipsed conformation is 104.2° (CASSCF), and for $[Os_2Cl_8]^{2-}$ it is in the range 105.0–106.2°, depending on the conformation and the computational level (SCF or CASSCF, see Table VI). Notice that a smaller pyramidality angle is expected for Os(IV) compounds at any level of computation, and this compensates in part for the shorter bond distance predicted with identical angles. The result is that the Os–Os quadruple bond is even slightly shorter than the corresponding triple bond, taken at their energy minima. All in all, the SCF and CASSCF optimized values of d and α are in fair agreement with the experimental data (Table VI). It is noteworthy that the optimized Os–Os bond distances are calculated to be quite similar for the Os(IV) compound (formally a quadruple bond) and the Os(III) compound (formally a triple bond) with the same pyramidality angle at both the SCF and CASSCF levels.

The importance of electron correlation can be analyzed by comparing the SCF and CASSCF results. The occupations of the σ^*, π^*, and δ^* orbitals calculated at the CASSCF levels for the quadruply bonded $[Os_2Cl_8]$ are plotted in Figure 15 as a function of the Os–Os distance, keeping the pyramidality angle constant (α = 105°). There it is seen that the σ^*- and π^*-orbitals contribute little to the ground state at bonding distances but become increasingly populated for long Os–Os distances, at which they lose a good part of their antibonding character. It is obvious that SCF calculations are inadequate to describe the dissociation of Os–Os bonds but are expected to yield reasonable results for small displacements of the Os atoms from their bonding distance. However, as the δ-orbitals have no influence on the $d(\alpha)$ relationship, the two configurations, $(\sigma)^2(\pi)^4(\delta)^2$ and $(\sigma)^2(\pi)^4(\delta^*)^2$, give analogous $d(\alpha)$ curves (not shown). The δ^*-orbital is not strongly antibonding because of the weak δ overlap, and an important contribution of the excited configuration $(\sigma)^2(\pi)^4(\delta^*)^2$ appears in the CASSCF ground state (see Figure 17). However, this does not affect the shape of the $d(\alpha)$ curve, as expected from the SCF results for the $(\delta)^2$ and $(\delta^*)^2$ configurations.

If the Os–Os distance is optimized for different pyramidality angles, the $d(\alpha)$ plots of Figure 17 result at the SCF (bottom) and CASSCF (top) levels. It may be seen once more that the metal–metal bond distance decreases for increasing pyramidality angles, although the dependence is far from being linear (see below). A stronger dependence is found for the smaller angles and a flatter curve for the larger ones. What is noteworthy of all these results is that the same qualitative trend is found at the EH, SCF, and CASSCF levels, which makes us more confident of the orbital hybridization discussed above for the Cr_2O_8 model compound. Notice also that the curves for the quadruple and triple bonds are almost coincident, indicating a small difference in bond lengths between the formal triple and quadruple M–M bonds with identical pyramidality angle and in agreement with our above conclusion that the pyramidality affects the σ and π components of the M–M bond, but not the δ one.

How Short Can a Metal–Metal Bond Be? In order to discuss this aspect, let us focus on the SCF results for $[Os_2Cl_8]^{2-}$ over a wider range of α (Figure 18). There one can distinguish roughly four regions of the $d(\alpha)$ curve: (i) a region with a strong negative slope for $\alpha < 100°$ (this corresponds to a positive slope in the $d(\cos\alpha)$ curve, structural parameter c in Table I); (ii) a region with a smaller negative slope ($100 < \alpha < 105°$); (iii) a plateau ($105 < \alpha < 115°$) with approximately constant Os–Os distance; and (iv) a region with a small positive slope at $\alpha > 115°$ (negative slope in $d(\cos\alpha)$, parameter c in Table I).

(64) Poumbga, C.; Daniel, C.; Bénard, M. *J. Am. Chem. Soc.* **1991**, *113*, 1090.

Table VI. SCF and CASSCF Results for $[Os_2Cl_8]^{2-}$ in the Eclipsed and Staggered Conformations and for $[Os_2Cl_8]$ in its Eclipsed Conformation, with Optimization of the Os–Os Bond Distance and the Os–Os–Cl Angle[a]

	eclipsed		staggered		difference (eclipsed – staggered)	
parameter	SCF	CASSCF	SCF	CASSCF	SCF	CASSCF
			$[Os_2Cl_8]^{2-}$			
total energy (a.u.)	−148.0029	−298.4798	−148.0072	−298.4848	0.0043	0.0050
Os–Os (Å) calcd	2.208	2.244	2.177	2.222	0.041	0.022
Os–Os (Å) exptl	2.210(2)		2.182(1)		0.032	
α(deg) calcd	106.2	105.8	105.5	105.0	0.7	0.8
α(deg) exptl	102.5–103.6		102.8–104.2		0.3–0.6	
			$[Os_2Cl_8]$			
Os–Os (Å) calcd	2.174	2.260				
α(deg) calcd	104.4	104.2				

[a] The Os–Cl distance was optimized only at the SCF level and kept constant (2.426 Å) at the CASSCF level. The large difference between the SCF and CASSCF energies results from the use of different pseudopotentials (see Methodological Aspects).

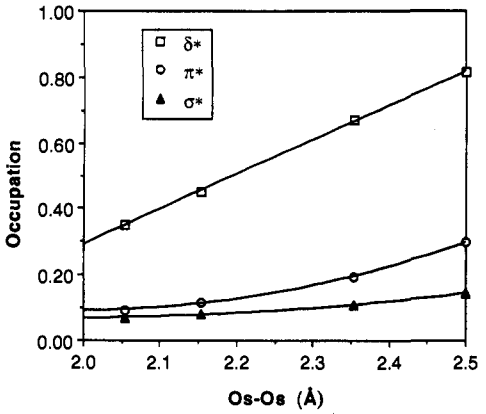

Figure 15. Populations of the M–M antibonding levels in $[Os_2Cl_8]$ calculated at the CASSCF level, indicating that electron correlation may be important for the δ-orbitals but very small for the σ- and π-orbitals.

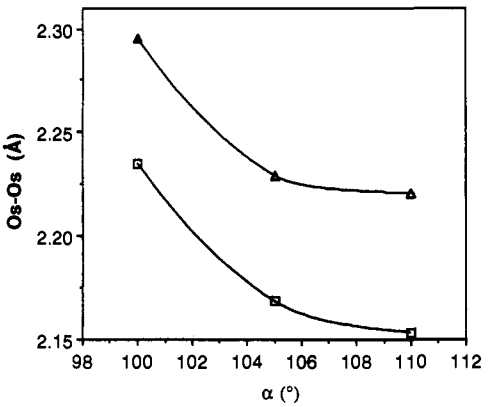

Figure 16. Calculated Os–Os bond distance as a function of the α angle in $[Os_2Cl_8]^{n-}$. □, $n = 0$ with the $(\sigma)^2(\pi)^4(\delta)^2$ configuration; △, $n = 0$ with the $(\sigma)^2(\pi)^4(\delta^*)^2$ configuration; both calculated at the SCF level.

Apparently, the fact that the different families of compounds in Table I show quite different susceptibility to pyramidalization could be related to the behavior shown in Figure 18: analogous curves can be expected for each particular family with the minimum at different angles, depending on factors yet to be determined. Since the experimentally available range of α for each family is relatively narrow, what we see in Table I, approximated by a linear expression, corresponds to only a small portion of the full $d(\cos\alpha)$ curve. That portion of the curve may correspond to one of the typologies i–iv noted above. Consider, for example, the sets of Mo(II) complexes. In Figure 19 we plot the Mo–Mo distances as a function of the pyramidality angle. The families of carboxylates and chelates, showing small angles, correspond to case i, with large negative slope. The carboxylatophosphine and halophosphine families, at larger angles, show little variation of the distance with α, corresponding to the plateau

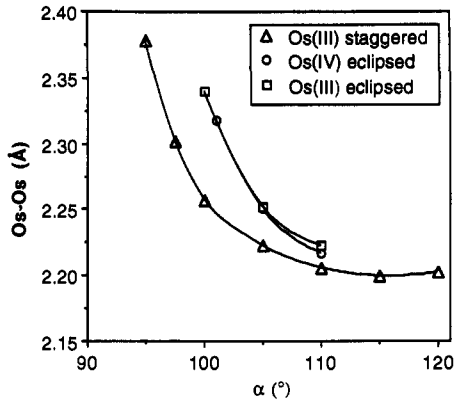

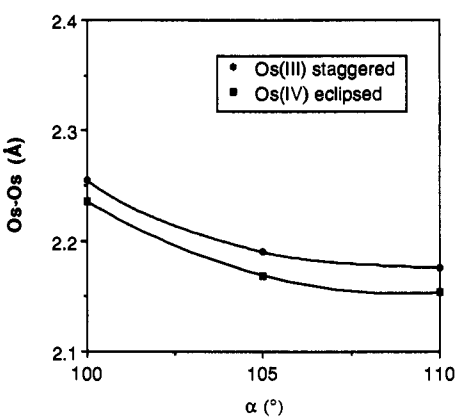

Figure 17. Calculated Os–Os bond distances as a function of the pyramidality angle α in complexes of the type $[Os_2Cl_8]^{n-}$, at the SCF (top) and CASSCF (bottom) levels. Os(III) ($n = 2$) corresponds to triple, Os(IV) ($n = 0$) to quadruple Os–Os bonds.

of iii or, in the case of the halophosphines, to a small negative slope (ii). Finally, the halodiphosphine complexes, at large angles, seem to have a small positive slope (iv). Here, however, the large dispersion of those points due to the differences in composition and rotation angles within the family makes the trend less evident (see, however, the clear-cut behavior of the subfamily of more closely related propyldiphosphine derivatives, Table I).

Effect of Axial Ligands. As additional chloride ligands are approached toward each Os atom in $[Os_2Cl_8]$, the pyramidality angle decreases as found previously in the extended Hückel calculations on the Cr model compound. In Figure 20 we represent the optimized pyramidality angle as a function of the Os–Cl_{ax} distance (SCF results). There it is seen that the approach of the axial ligands forces smaller pyramidality angles for the equatorial ones, on their way to an octahedral coordination geometry for Os. The Os–Os bond length, also optimized for each Os–Cl_{ax} distance, is again clearly dependent on α.

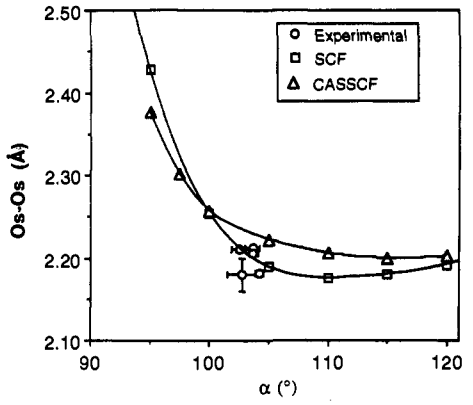

Figure 18. Dependence of the Os–Os bond distance on the pyramidality angle α for $[Os_2Cl_8]^{2-}$ in the staggered conformation, calculated at the SCF (□) and CASSCF (△) levels. Experimental values (○) for several salts of this anion are also plotted for comparison.

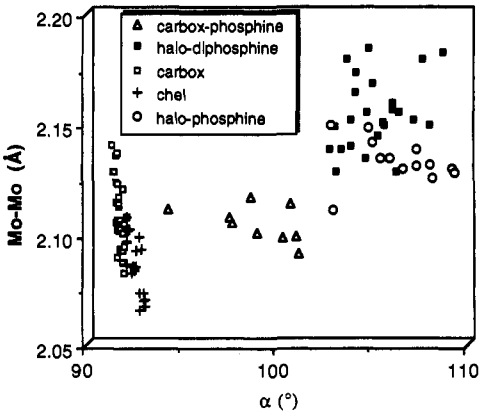

Figure 19. Plot of the experimental Mo–Mo distances as a function of the pyramidality angle α for several families of Mo(II) compounds.

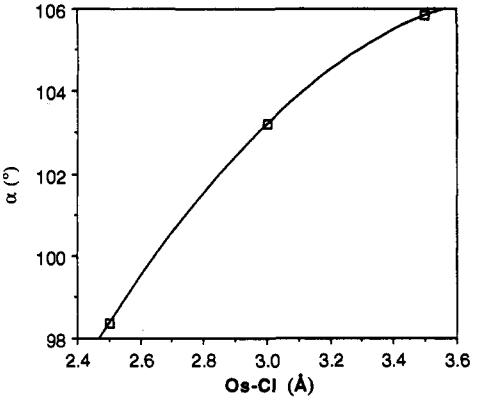

Figure 20. Optimized pyramidality angle α in $[Os_2Cl_{10}]^{2-}$ as a function of the Os–axial ligand internuclear distance (SCF results).

Internal Rotation in Systems with Triple Bonds. Let us now look for an explanation of the correlation between internal rotation angle χ and M–M bond distance in triply bonded compounds of Tc, Re, and Os. Such a correlation shows up also in the MO calculations carried out for the $[Os_2Cl_8]^{2-}$ ion at extended Hückel, SCF, and CASSCF levels, even if no barrier to internal rotation associated with π-bonding is expected in M_2X_8 compounds[65] because of the degeneracy of the π-orbitals. The total energy appears to decrease with the internal rotation angle χ (Table VI). The calculated energy difference between both conformations is 2.7 and 3.1 kcal/mol at the SCF and CASSCF levels, respectively, and the Os–Os bond distance is calculated to be 0.041- and 0.022-Å shorter in the staggered case, in good agreement with an experimental difference of 0.032 Å.

It is easier to trace back the origin of such effects at the orbital level by using extended Hückel calculations on the same ion and analyzing the Os–Os overlap population. It increases from 0.805 in the eclipsed to 0.821 in the staggered conformation (compare with an increase of 0.055 in the overlap population produced by a δ-bond). The effect of a $d_{x^2-y^2}/d_{xy}$ interaction between the approximately planar MX_4 fragments suggested by Kryuchkov *et al.*[6] (**6**) contributes only 0.001 to the increase in Os–Os overlap

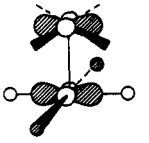

6

population, because the $d_{x^2-y^2}$ orbital interacts strongly with the σ-donor orbitals of the ligands but very poorly with d_{xy} of the other metal atom.

What is the reason, then, for such a small, yet significant, bond strengthening? The overlap population analysis indicates that four-electron repulsions in the eclipsed conformation are avoided by internal rotation; these repulsions derive in approximately equal proportions from the p_z lone pairs of the halide ligands (**7a**) and the σ(M–X) bonding pairs (**7b**). An analysis of the theoretical

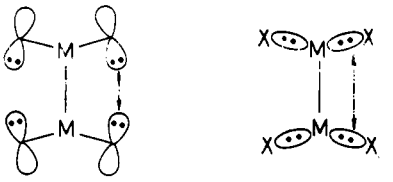

a b

7

and experimental data supports this explanation: the SCF and CASSCF geometry optimizations yield a slightly smaller OsOsCl angle for the staggered case, suggesting that the Cl···Cl repulsions force it to open in the eclipsed conformation. On the other hand, the longer M–M bond distances found for the smaller halide ligands in the eight-electron series $[Re_2X_8]^{2-}$ (Table VI) can also be attributed to such *steric* repulsions.

If the calculated barrier of rotation for $[Os_2Cl_8]^{2-}$ (2–3 kcal/mol) is a reasonable estimate, solutions of this and related anions should show dynamic behavior which might be experimentally detectable with an adequate selection of ligands. On the other hand, the small barrier accounts for the existence of compounds with different angles χ, since *packing forces* may be as important as the intramolecular ligand···ligand repulsions and could favor one or another conformation. Let us remark that the computed barrier for internal rotation is comparable to that associated with a δ-bond in 8-electron complexes, which has been calculated for $Re_2Cl_8^{2-}$ as 3.0 kcal/mol.[66]

4. Methodological Aspects

Extended Hückel Calculations. All the molecular orbital calculations of the extended Hückel type[67] were carried out using the modified Wolfsberg–Helmholz formula[68] and the atomic parameters shown in Table VII. The following bond distances

(65) Campbell, F. L.; Cotton, F. A.; Powell, G. L. *Inorg. Chem.* **1984**, *23*, 4222.

(66) Smith, D. C.; Goddard, W. A. *J. Am. Chem. Soc.* **1987**, *109*, 5580.
(67) Hoffmann, R. *J. Chem. Phys.* **1963**, *39*, 1397.
(68) Ammeter, J. H.; Bürgi, H.-B.; Thibeault, J. C.; Hoffmann, R. *J. Am. Chem. Soc.* **1978**, *100*, 3686.

Table VII. Atomic Parameters for Extended Hückel Calculations[a]

atom	orbital	H_{ii}	$\zeta_{1\mu}$ (c_1)	$\zeta_{2\mu}$ (c_2)	ref
Cr	4s	−8.66	1.70		
	4p	−5.24	1.70		
	3d	−11.22	4.95 (0.5060)	1.80 (0.6750)	72
Os	6s	−8.17	2.452		
	6p	−4.81	2.429		
	5d	−11.84	5.571 (0.6372)	2.416 (0.5598)	73
O	2s	−32.3	2.20		
	2p	−14.8	1.975		
Cl	3s	−30.0	2.183		
	3p	−15.0	1.733		
H	1s	−13.6	1.300		67

[a] $H_{\mu\mu}$'s are the orbital ionization potentials, $\zeta_{i\mu}$ the exponents of the Slater orbitals, and c_i the coefficients in the double-ζ expansion of the d orbitals.

were used and kept constant throughout: Cr–Cr = 2.30; Cr–O = 2.01; Os–Os = 2.12; Os–Cl = 2.31; and Os–H = 1.69 Å.

Ab Initio Calculations. *Ab initio* calculations at different computational levels (SCF, CASSCF) were performed for $[Os_2Cl_8]$ in its eclipsed conformation and for $[Os_2Cl_8]^{2-}$ in both the eclipsed and the staggered conformations. At each computational level the Os–Os bond distance and the Os–Os–Cl bond angle were optimized. The Os–Cl bond distance was first optimized at the SCF level, and the optimized value (2.426 Å) was kept constant.

In all calculations we employed effective core pseudopotentials (ECP) to replace the core electrons of the Cl and Os atoms.[69] In the set of pseudopotentials used for our calculations, 5s, 5p, 6s, 6p, and 5d orbitals were included in the basis set and the innermost orbitals were frozen. The SCF calculations were all performed with large core pseudopotentials in which also 5s and 5p orbitals were frozen. The CASSCF results predict longer Os–Os bond distances than SCF calculations, a result which could be anticipated.[70] CASSCF calculations carried out with the small core lead to shorter distances and somewhat larger bond angles, in excellent agreement with experimental data (Table VI). Therefore, only small core CASSCF results are discussed throughout this paper, except for the correlation energy resulting from the comparison of SCF and CASSCF calculations with the same set (large core) of pseudopotentials (calculated correlation energy = 0.18 hartrees).

The primitive Gaussian basis set used to represent the valence orbitals[71] was (3s,3p,3d) contracted to [2s,2p,2d] for Os and (3s, 3p) contracted to [2s, 2p] for Cl. As a check, diffuse functions were included in a calculation for $[Os_2H_8]^{2-}$, (4s, 4p, 4d) contracted to [3s, 3p, 3d] and (5s) contracted to [3s] for Os and H, respectively, but the qualitative results remained unaltered and only small differences in the calculated rotational barrier were found. As a consequence, we consistently used a basis set with a frozen core and no diffuse functions. For a detailed discussion of the methodological aspects and the importance of electron correlation in systems with M–M multiple bonds, the reader is referred to the earlier papers of Bénard[56] and Hay[58] and to a recent account by Bénard and co-workers.[55]

Acknowledgment. The research at Barcelona was supported by CICYT through grant PB89-0268. Allocation of computer time at the *Centre de Supercomputació de Catalunya* (CESCA) was possible thanks to an EASI project funded by IBM-España. The authors are indebted to S. Gambarotta, M. H. Chisholm, and F. A. Cotton for sending to us preprints of their work, to M. Bénard and P. Alemany for enlightening discussions, and to F. Vilardell for the drawings. The authors are grateful to R. Reina, who first suggested to us that we should consider pyramidality during her study of semibridging carbonyl clusters.[74]

Supplementary Material Available: Tables of structural data for the Cr(II), Mo(II), W(II), Re(III), and Os(III) chelates and complexes studied, including references to the literature (29 pages). Ordering information is given on any current masthead page.

(69) Hay, P. J. *Chem. Phys. Lett.* **1984**, *103*, 466. Hay, P. J.; Wadt, W. R. *J. Chem. Phys.* **1985**, *82*, 270.
(70) Roos, B. O. *Adv. Chem. Phys.* **1987**, *69*, 399.
(71) Dunning, J. *J. Chem. Phys.* **1970**, *53*, 2823.
(72) Summerville, R. H.; Hoffmann, R. *J. Am. Chem. Soc.* **1976**, *98*, 7240.
(73) Jørgensen, K. A.; Hoffmann, R. *J. Am. Chem. Soc.* **1986**, *108*, 1867.
(74) Alvarez, S.; Ferrer, M.; Reina, R.; Rossell, O.; Seco, M.; Solans, X. *J. Organomet. Chem.* **1989**, *377*, 291.